OCTOBER 1979 LRP 151/79

PRELIMINARY RESULTS FROM A 66 μm D_2O LASER HAVING AN UNSTABLE RESTSTRAHLEN RESONATOR

M.R. Green, I. Kjelberg, P.D. Morgan,
M.R. Siegrist, R.L. Watterson, and E. Akhmetov

PRELIMINARY RESULTS FROM A 66μm D_2O LASER HAVING AN UNSTABLE RESTSTRAHLEN RESONATOR

M.R. Green, I. Kjelberg, P.D. Morgan
M.R. Siegrist, R.L. Watterson, and E. Akhmetov*

Centre de Recherches en Physique des Plasmas
Association Euratom - Confédération Suisse
Ecole Polytechnique Fédérale de Lausanne
21, Av. des Bains, CH-1007 Lausanne, Switzerland

*on attachment from
Department of Optics and Spectroscopy
University of Kazakhstan
ALMA ATA, U.S.S.R.

Abstract

Most ionic crystals have strong reflection bands in the far infrared. Many such crystals are also transmissive to infrared radiation. We describe an unstable resonator that exploits these properties. Preliminary results from a device 134 cm long and of 6 cm diameter are presented. For a pump pulse of 10 Joules and of duration 75 nanoseconds output powers of 0.7 megawatts have been measured. A correlation between the mode beating of the pump wave and the FIR wave it generates is demonstrated.

1. Introduction

Most ionic crystals have strong reflection bands in the far infrared (FIR) region of the electromagnetic spectrum. The phenomenon, termed reststrahlen reflection, {1} is due to a resonant absorption and re-emission of the incident radiation by the crystal lattice ions. We have previously drawn attention to an additional property of many reststrahlen crystals, that of being highly transmissive to infrared radiation and, consequently, to their possible use in optically-pumped FIR lasers {2}. In particular, we proposed the use of an unstable resonator for the 66μm line of D_2O in which a plate of KCl simultaneously acts as a low-loss window to the 9.66μm pump radiation from the CO_2 laser, and as a reststrahlen mirror to the FIR radiation. In this report, we describe preliminary results obtained at 66μm using such a resonator, together with results obtained using a plane-plane resonator in which one mirror was a reststrahlen crystal and the output coupler was a wire mesh.

2. Apparatus

a) The CO_2 Laser System

The CO_2 laser system used to optically pump the D_2O lasers is described in detail elsewhere {3}, but a brief account is given here. The system figure (1), comprises 5 identical TEA laser modules, the construction of which is described in {4}. Each module, of discharge volume 100x5x5 cm, is capable of outputs in excess of 60 J, when run as an oscillator at 10.6μm. We use one module as an oscillator and the remainder as amplifiers. The 240 cm long oscillator cavity comprises a diffraction grating (150 grooves per mm and blazed for 8μm), and a ZnSe meniscus output coupler coated to give a reflectivity of 55%. The half-symmetric resonator produces a single transverse-mode when an aperture of 8 mm is placed in front of the grating. In order that the oscillator produces a single axial mode, and that it may be tuned off line-centre there is provision

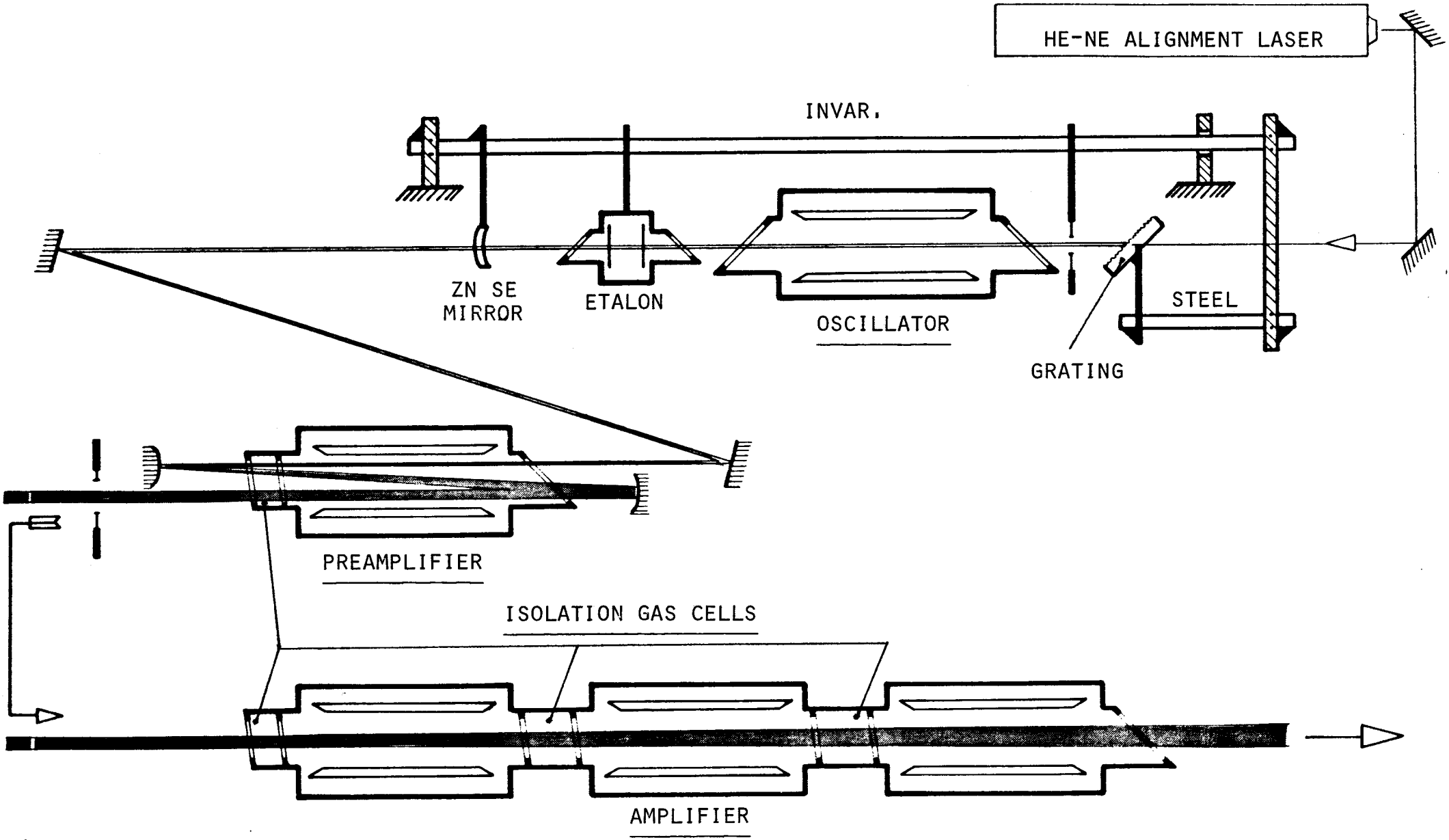

ø = 45 mm

E = 25 JOULES (for λ = 9.66 µm)

Fig. 1 CO_2 laser system for optical pumping

for an etalon to be inserted into the cavity. The use of an intra-cavity etalon implies that the overall cavity length must not vary by more than a small fraction of λ. Consequently, the resonator support structure is temperature compensated; this is achieved by opposed steel and invar spacers. When the ratio of the lengths of the steel and invar is the inverse of the ratio of the expansion coefficients, then the expansion of the steel counteracts the expansion of the invar {5}. For the experimental work to be described in this report the etalon was not used; thus the output of the CO_2 oscillator contained several longitudinal modes. The 0.3 Joule, 8 mm diameter beam passes via a beam steerer into the triple-pass preamplifier. An off-axis Cassegrainian telescope is used to expand the beam whilst it is being amplified. On leaving the pre-amplifier, the 45 mm diameter beam makes a single pass through the final three modules. Energies of up to 25 Joules can be achieved from the whole chain. To isolate the modules from each other and to prevent the build-up of parasitic oscillations four gas cells are used. A mixture of 3 gases, viz. CF_2Cl, C_4F_8 and SF_6, at a total pressure of about 10 torr, is used so that transmission of 9.66μm radiation through the cells is high (>95%) whilst for most other possible lasing wavelengths it is small (<10%). A typical ir-spectrum of the gas mix transmission is shown in figure (2).

Further details of the properties of this gas mix and the technique used for its optimisation can be found in reference {6}.

The length of the output pulse can be chosen within the range 50 ns to 2.5 μs simply by altering the timing between firing the oscillator and amplifier stages, that is, by choosing to amplify the spike alone or progressively more and more of the tail. Figure (3) shows some oscilloscope traces of the final output pulse shape as a function of the time delay between firing oscillator and amplifier.

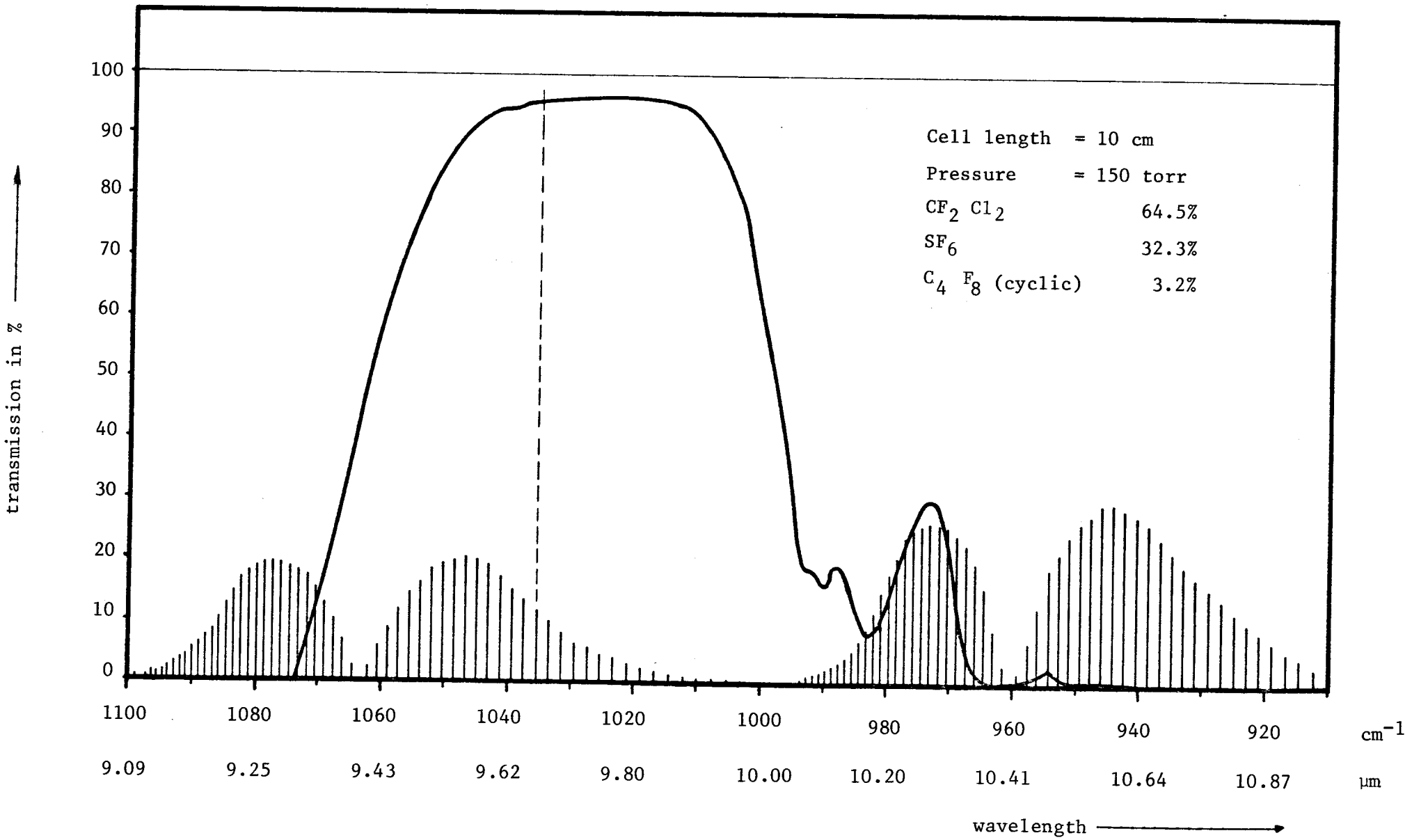

Fig. 2: A typical IR spectrum of the isolation gas-cell mix;
also shown relative gain of P and R branch CO_2 laser transitions.

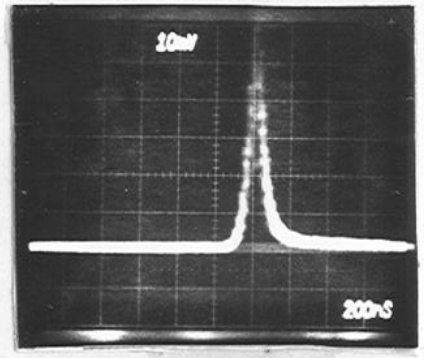

ΔT = 0 μsec

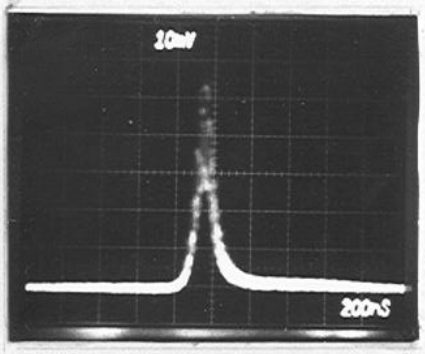

ΔT = 0.4 μsec

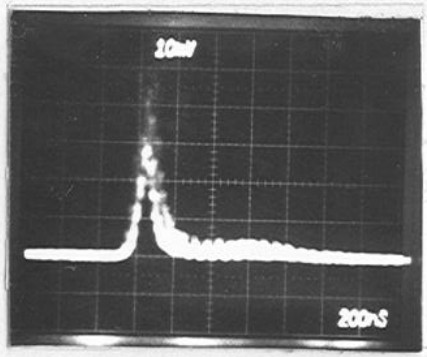

ΔT = 0.8 μsec

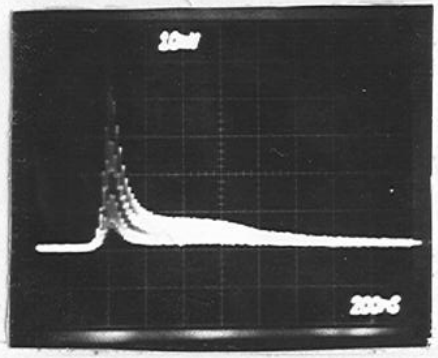

ΔT = 1.2 μsec

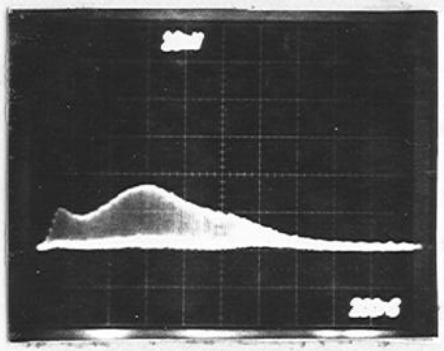

ΔT = 1.6 μsec

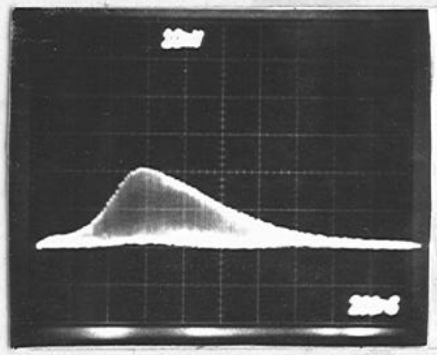

ΔT = 2.0 μsec

Fig. 3 Temporal output of CO_2-Laser system as a function of delay between oscillator and amplifiers

Vertical scale : 10 mV/Div.

Horizontal scale: 200 ns/Div.

b) The Unstable Reststrahlen Laser Resonator

For single-transverse-mode oscillation from high-power large-diameter lasers, the unstable optical resonator has many attractive properties {7}. Using such a resonator, excellent transverse-mode selection and optimal output coupling may be achieved using all-reflective optics.

In figure (4), the unstable resonator oscillator for 66 μm, which utilizes the reststrahlen effect, is shown. The CO_2 laser radiation enters the oscillator through a KCl plate, which has a high damage threshold to the radiation, set at 45^o (reflection losses are low since this is close to the Brewster angle of 55^o). The resonator comprises a concave, gold coated mirror and a KCl element, the inner surface of which is convex and acts as a reststrahlen mirror to 66μm radiation. By making the radius of curvature of both surfaces of the element the same, the pump beam is not diverged on passing through it. An amplifier section can be readily added to the oscillator, as shown in the figure.

Because of the transparency of the KCl element to the 9.66μm radiation the sensitive central section of the D_2O resonator, where the FIR single mode builds up, is uniformly pumped. This would not be the case when an output coupler which is opaque to the pump radiation is used. For this latter case, pump energy can be coupled into the obscured region by Fresnel diffraction around the mirror. However, in general, this technique is not satisfactory because a highly non-uniform radial distribution of pump energy, and consequently of the FIR gain, occurs. We illustrate this by means of beam propagation calculations which include diffraction {8}. Consider an unstable resonator of length 150cm, beam diameter 6cm and output coupling 50%; figures (5a) and (5b) show the distribution of pump energy as a function of radius and distance along the axis from the output coupler for a KCl-restrahlen (92% transmission) and opaque mirror, respectively. From the point of view of uniform pumping the latter case is clearly inferior.

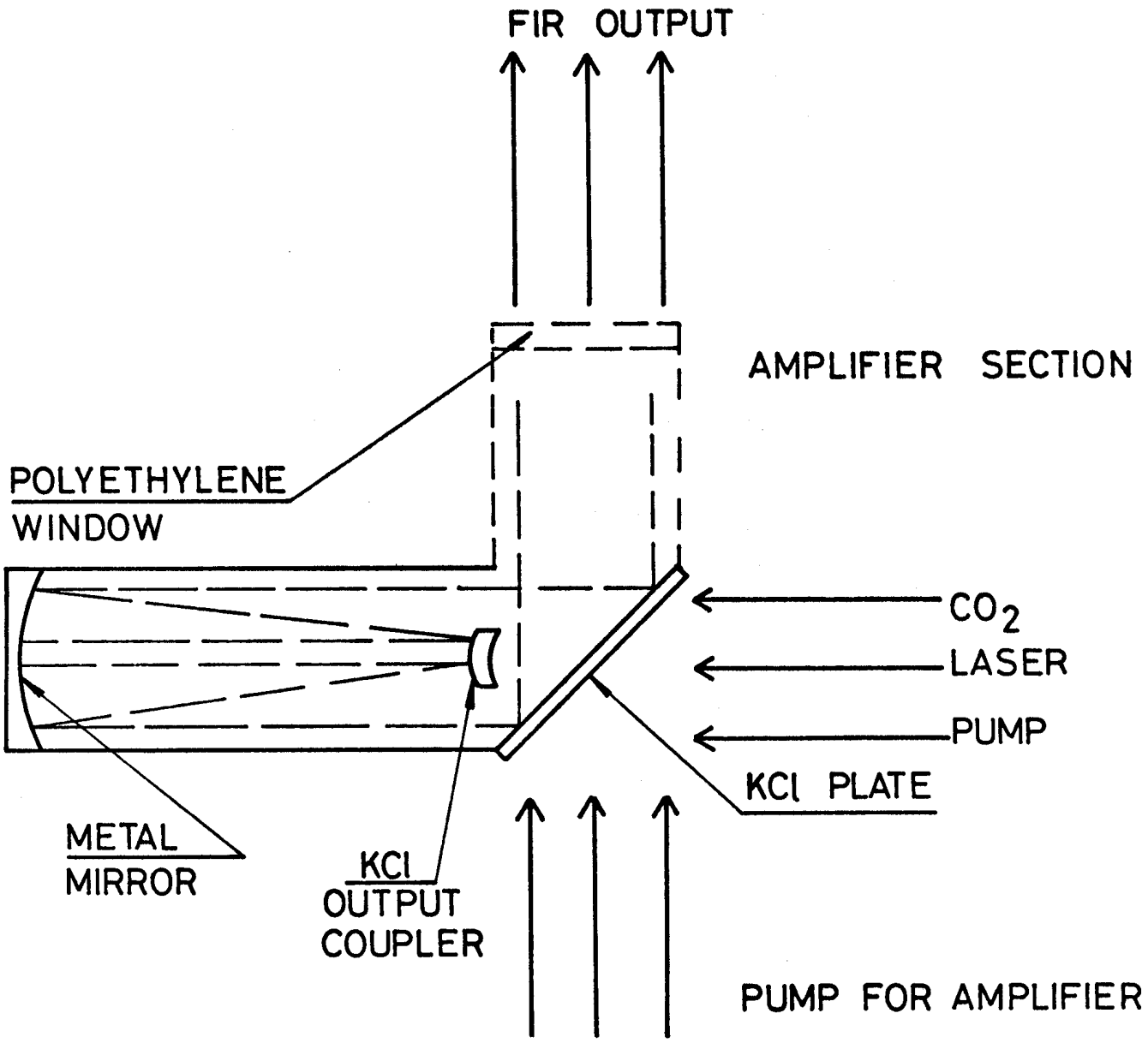

Fig. 4 An unstable resonator which utilises the reststrahlen effect

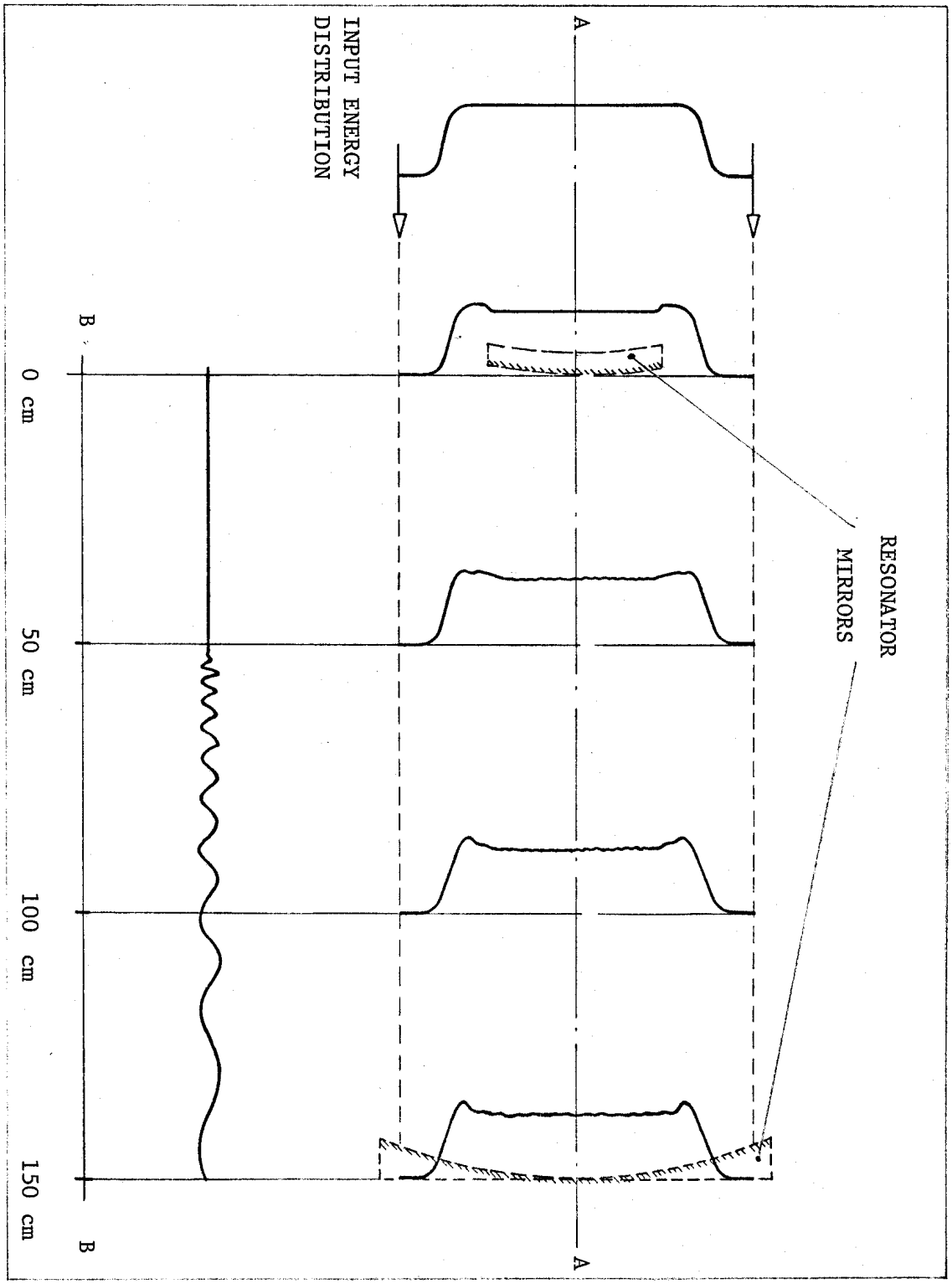

Fig. 5a: Distribution of pump energy: with a restrahlen mirror

A - A Radial Variation

B - B On-Axis Variation

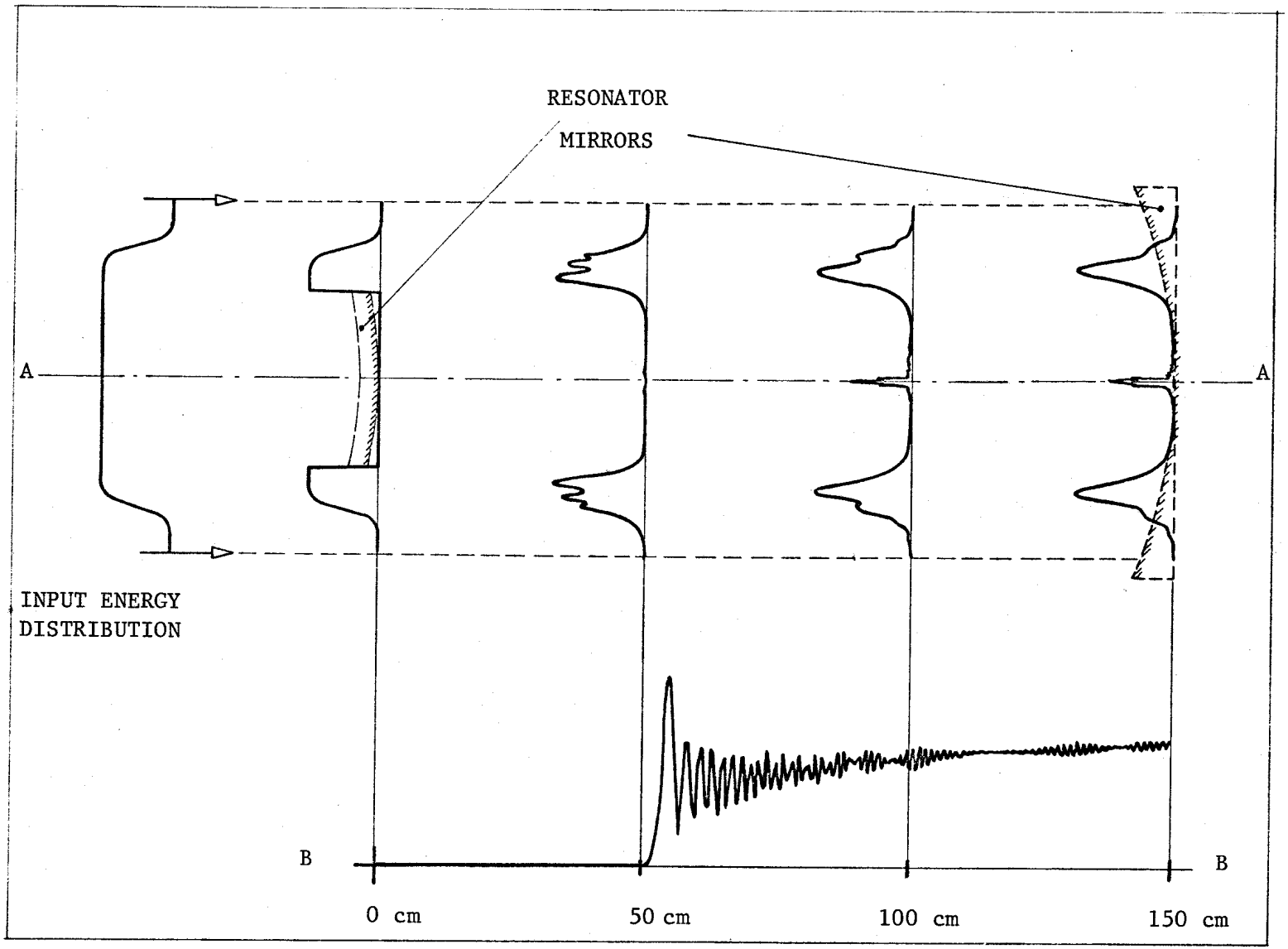

Fig. 5b: Distribution of pump energy: with an opaque mirror.

A - A Radial Variation

B - B On-Axis Variation

3. Results

Prior to the use of the unstable resonator, a number of uncertainties required clarification. These were : whether or not KCl, which is hygroscopic, can withstand long-term immersion in an atmosphere of D_2O at a pressure of a few torr, whether the reststrahlen reflectivity of KCl at 45^o differs significantly from the published value of 88% at normal incidence and whether reflectivity decreases at high irradiance, i.e. whether the reststrahlen effect saturates.

The simple plane-plane resonator configuration used to investigate the above points is illustrated in figure (6). It comprised a KCl reststrahlen reflector and a wire mesh output coupler. The reflectivity of the output coupler could be changed by using meshes of different spacing. Only a limited range of such meshes is commercially available {9}.

l.p.mm.	Nominal aperture (μm)	Transmission,T, at 66 μm ($151\ cm^{-1}$) ± 5% (measured)	Reflectance R, = 1 - T
59.1	11	0	100
39.4	18	7.5	92.5
29.5	26	42	58
23.6	33	73	27
19.7	41	91	9
16.9	49	95-100	0-5

Table I

Measured transmission of commercially available meshes

Measurements performed by Prof. J.C. Bünzli, University of Lausanne, using a Bruker IFS-113c infrared Fourier spectrometer.

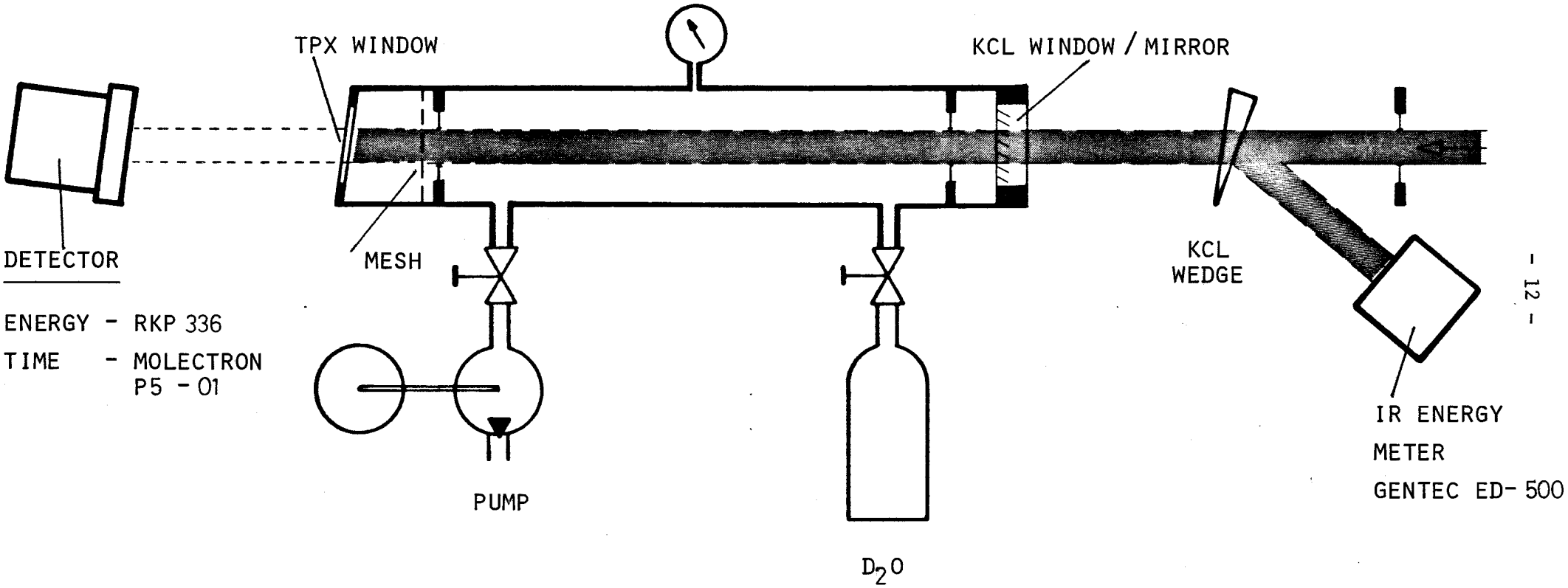

Figure 6 The linearly pumped D_2O laser oscillator.

Table I lists mesh spacing and the measured transmission, T, of the meshes at 66μm, together with an estimate of the reflectance, assuming R = 1-T. The cavity was linearly pumped through the KCl reflector, the FIR output being obtained by means of a TPX window beyond the mesh. Although TPX transmits fairly well at 66μm, it absorbs very strongly at 9.6μm (10). Consequently the output contains only FIR radiation. The KCl reflector suffered no damage after many hours of continuous exposure to D_2O vapour at pressures up to 10 torr.

The output from the simple oscillator was used to measure the reflectivity of KCl at 45°. Within the experimental error of ±10%, the reflectivity was the same as for normal incidence, i.e., 88%.

In figure (7a) we plot the FIR energy output as a function of D_2O vapour pressure, for a number of different meshes. The FIR energy was measured using a RkP 336 pyroelectric detector, with an extended spectral response. By cross checking its calibration with that of two other detectors, the uncertainty in the values of energy given are estimated as 25% (appendix I). The pump pulse was of energy 8J and of duration 75ns FWHM. The maximum output energy occurs at a pressure of about 7 torr, for any mesh. For the sake of completeness, the case with the output coupler removed* is also shown.

The conversion efficiency (FIR laser energy/CO_2 laser energy) of the D_2O laser can be influenced by the past history of the laser's vacuum vessel (see Appendix II). Consequently care has been taken to 'condition' the vessel surfaces and to perform calorimetry shortly following a fresh charge of vapour as the efficiency is then at its highest and most reproducible.

*The gain of FIR lasers is generally quite high and therefore a laser resonator is not required to produce FIR laser emissions. All that is needed is a long tube with a window on one end transparent to the pump radiation, and a window at the other end transparent to the FIR radiation. Laser emissions can occur because some spontaneous emission is amplified by the high gain of the medium in one pass through the tube. This type of laser action is often called amplified spontaneous emission (ASE). However, the results of some recent experiments have suggested that a related phenomenon, Dicke superradiance {11}, may be responsible for this emission. To distinguish between these two species will require further experimentation.

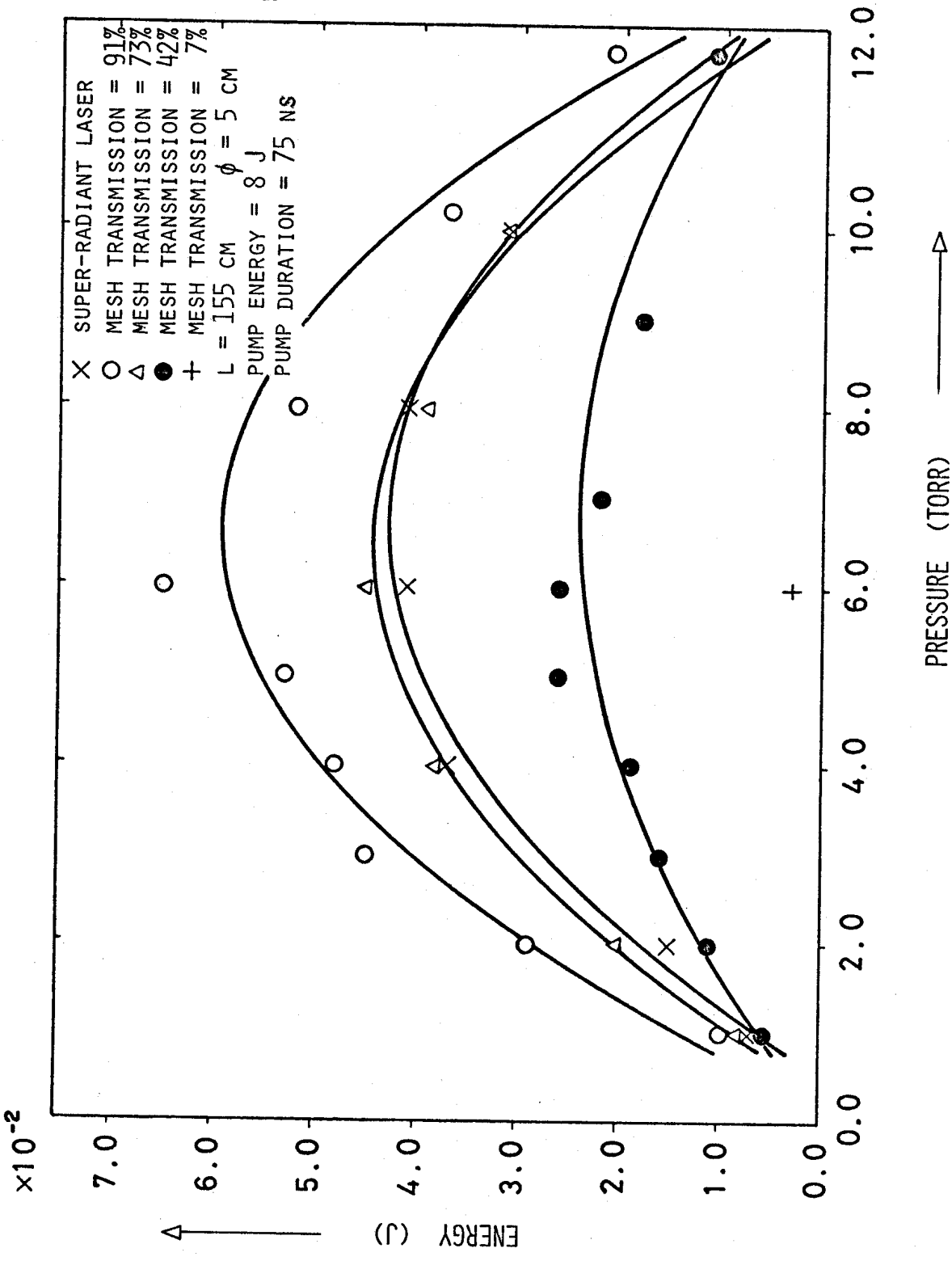

Fig. 7a: FIR energy as a function of D_2O vapour pressure: plane/plane resonator.

The peak energies shown in figure (7a) are replotted in figure (7b) as a function of mesh reflectivity. It is not possible to define the function with any real confidence, owing to the limited data. The dotted line, however (fitted by eye), suggests that optimum efficiency is obtained when $5 < R < 15\%$. We have calculated the optimized reflectivity as a function of localized losses, based on a coupled three-level system (including single and double photon transitions) {12} and obtain a reasonable agreement with these results.

Figure (8) shows the FIR output energy as a function of CO_2 laser energy, for a D_2O vapour pressure of 6 torr, for pump pulses of duration 75 ns and 1.5 μs. The relationship is linear up to a pump energy density of 0.35 J/cm, and is independent of the pulse duration within these limits.

The FIR pulse-shape was recorded using a Molectron P5-01 pyroelectric detector (frequency bandwidth 700 MHz) and a Tektronix 7904 oscilloscope mainframe in conjunction with a 7A 19 plug-in unit (combined frequency bandwidth 500 MHz at 10 mV/cm. Figure (9) shows a typical pulse-shape. No appreciable delay was measured between the pump wave and the FIR output it generated. The modulation of the waveform arises partly from the well-known effect of mode-beating, the period, τ, corresponding to the cavity round-trip time, i.e., $\tau = 2L/c$, L being the cavity length. For the cavity length of 155 cm the period is 12.3 ns. A rather interesting feature of these measurements was that without a cavity the ASE alone exhibited a pronounced, regular modulation of 16 ns period, figure (10a). Furthermore with more careful examination beats with this period were found to persist even with cavity feedback, figure (9), in superposition with that due to the FIR cavity. The 16 ns period corresponds to the round-trip time of the 240 cm long CO_2 laser oscillator, figure (10b). We attribute this temporal correlation to the presence of near resonant stimulated Raman emission from each frequency component of the pump {13}. Thus the FIR output, figure (9), comprises FIR laser modes which correspond to the FIR cavity resonances, together with superradiant emission the frequency difference of which corresponds to that of the CO_2 laser modes. All these frequencies mix at the detector to produce the traces shown in the figures.

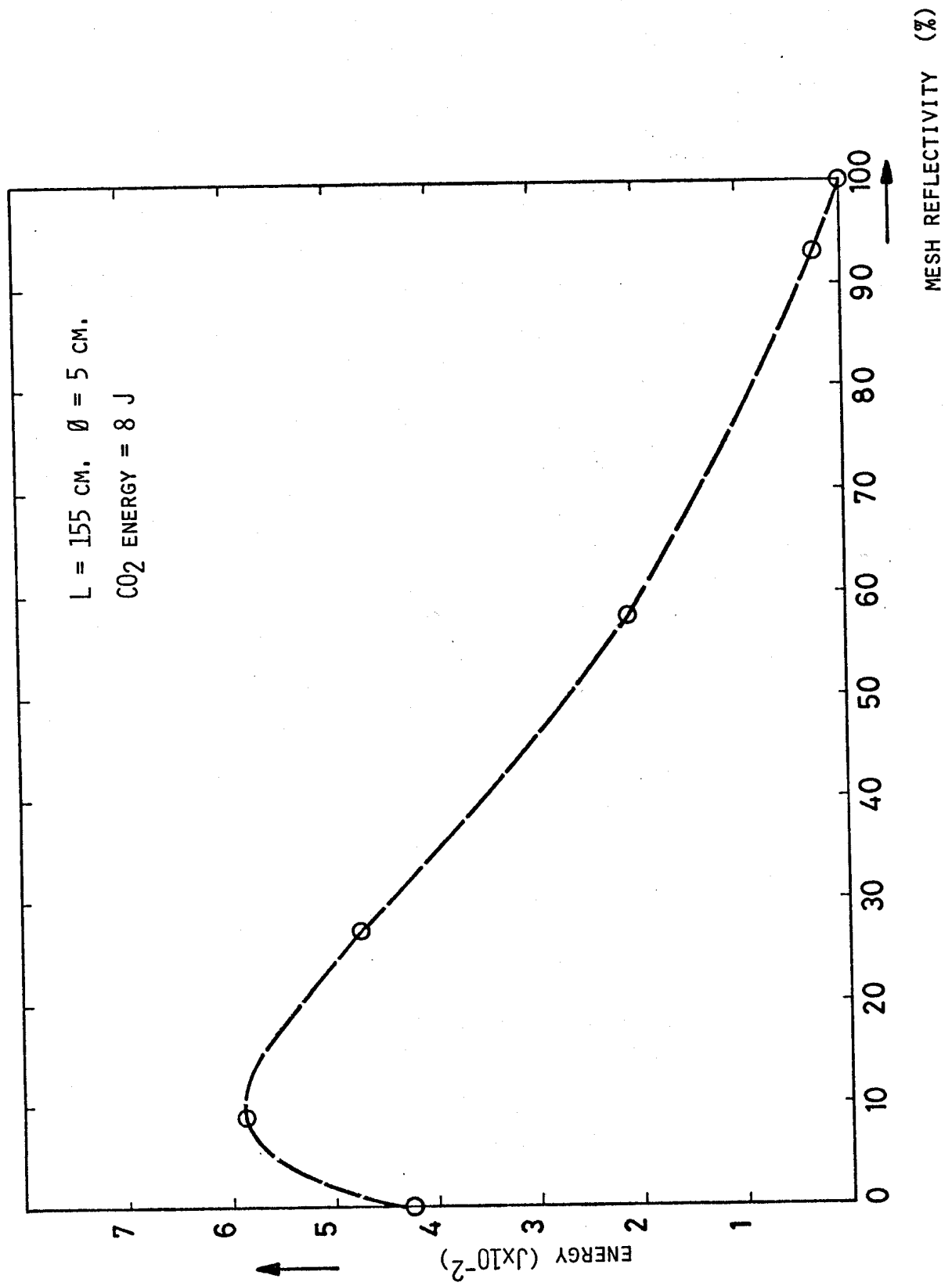

Fig. 7b: Maximum energy output from the FIR oscillator as a function of mesh reflectivity: plane/plane resonator.

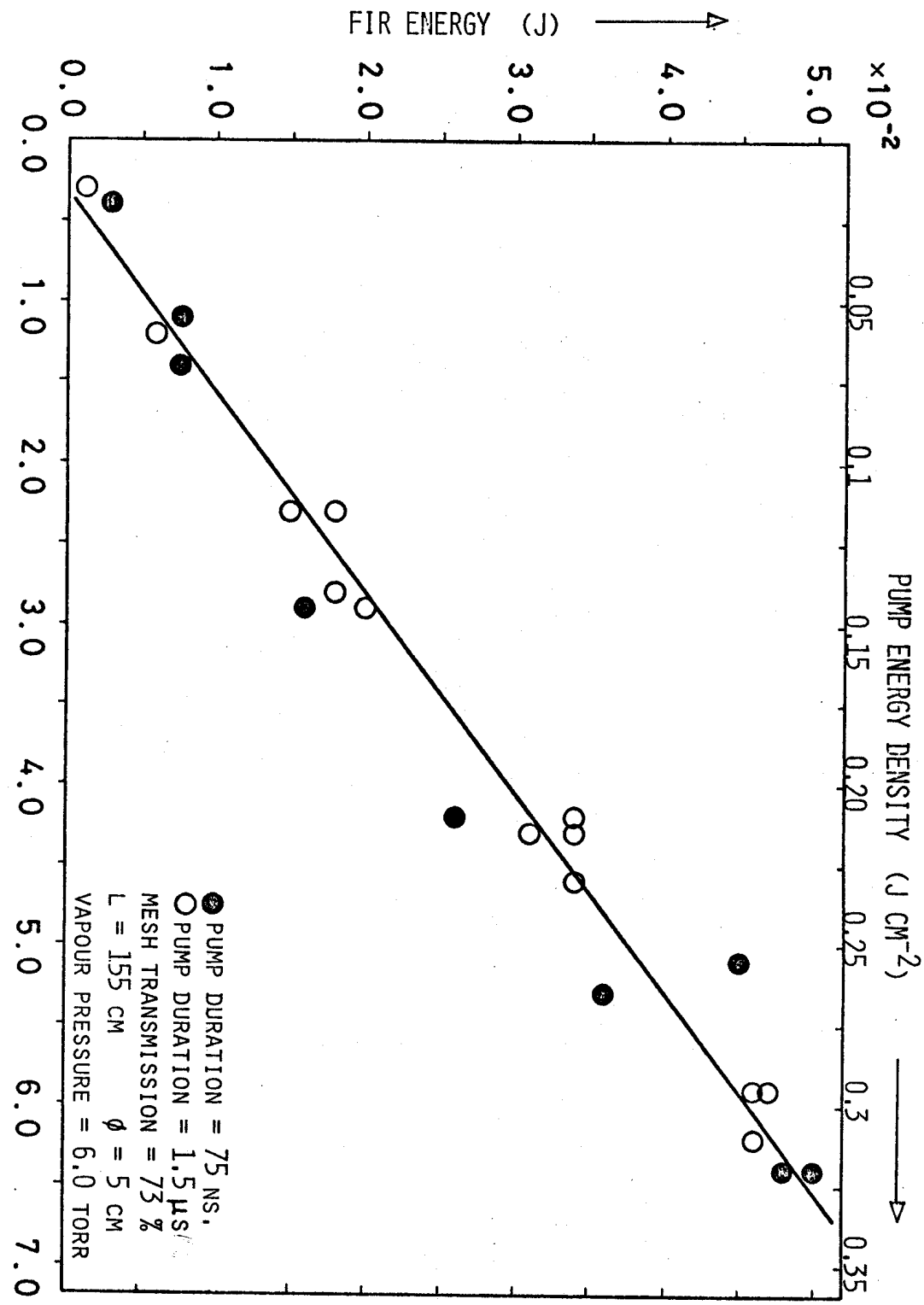

Fig. 8: FIR energy as a function of CO_2 laser pump energy for two pump durations: plane/plane resonator.

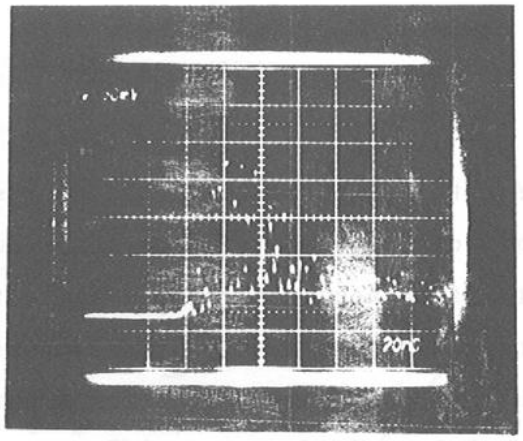

Fig. 9

A typical FIR pulse shape.

Plane/plane cavity.

L = 155 cm.

R = 27%

20 ns/div.

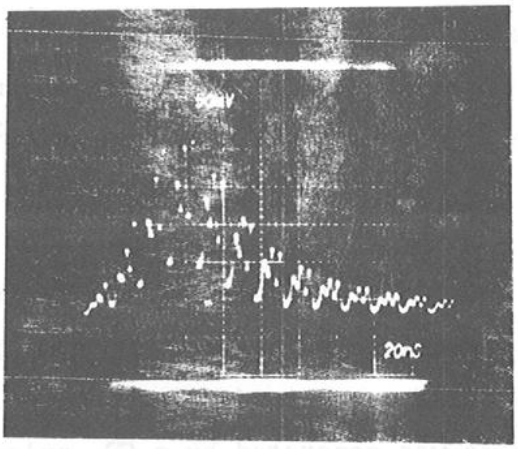

Fig. 10a

FIR pulse shape : ASE

20 ns/div.

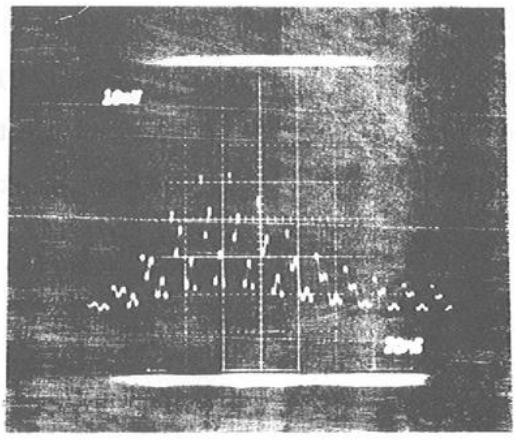

Fig. 10b

CO_2 pump pulse shape

20 ns/div.

CO_2 cavity length : 240 cm.

We now consider the results obtained using the unstable resonator. The resonator length was 134 cm and beam diameter 6 cm. The output coupling was set to 56%, the resonator feedback was 32%, and reflection losses 12%. In figure (11) we plot the output energy of the unstable resonator at 66μm as a function of the D_2O vapour pressure, for a pump pulse of energy 8 Joules and duration 1.5 μs FWHM The maximum output occurs at a pressure of about 7 torr. Under otherwise identical conditions, but with pump pulses of 75 ns FWHM, no appreciable difference in the FIR energy was recorded.

Figure (12) shows the dependence of the FIR output on the CO_2-pump energy, at a constant pressure. A linear relationship is in good agreement with the experimental points. Even at the maximum pump energy of 10 J, corresponding to an energy density of 0.35 Joules/cm^2, there is no evidence of saturation.

In figure (13a) and (13b), the pulse waveforms of two typical FIR pulses are reproduced; for comparison the corresponding CO_2-pump pulses are shown above. The first FIR pulse corresponds to a pump pulse duration of 75 ns FWHM, while the second was generated by a CO_2 pulse approximately ten times longer. As before, the modulation of the pulse envelope has two periods, one corresponding to the cavity round-trip time and the other to the modulation of the pump due to mode beating. The FIR pulse duration always slightly exceeded that of the CO_2 pump.

Because the FIR laser cavity was neither thermally nor mechanically stable, we did not measure the frequency spectrum of the FIR output. A scanning Fabry-Perot interferometer requires about 100 shots to construct a spectrum, and during the time taken for this number of shots ($\sim 1\frac{1}{2}$ hrs) the overall cavity length would vary by more than λ.

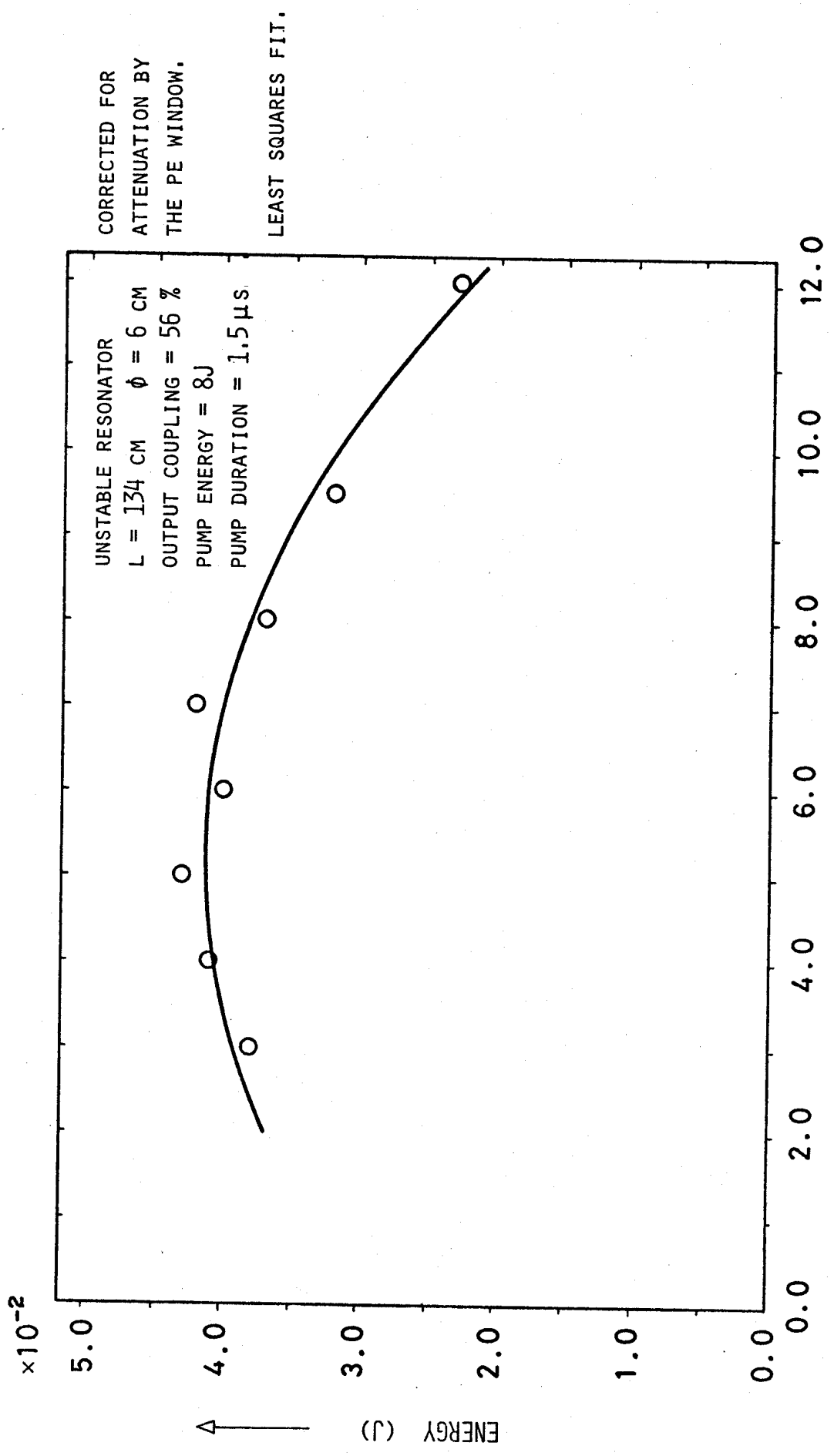

Fig. 11: FIR energy as a function of D_2O vapour pressure: unstable resonator

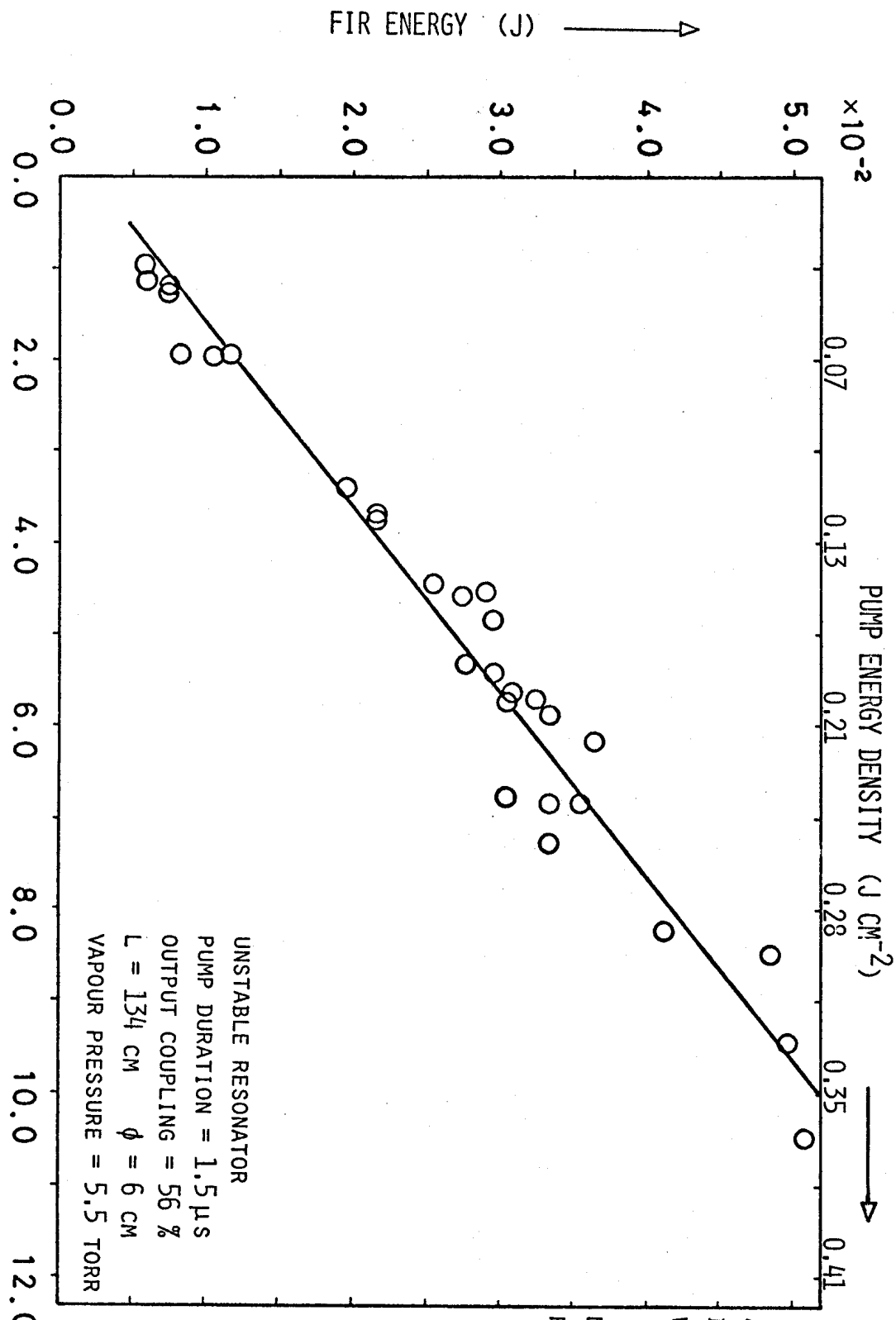

Fig. 12: FIR energy as a function of CO_2 pump energy: unstable resonator

A. "SHORT PULSE"

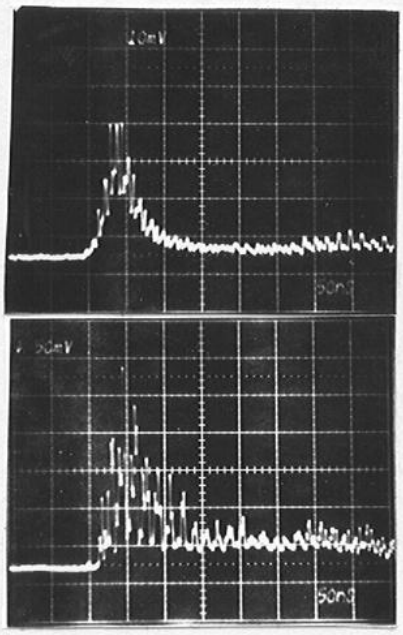

I CO_2 Pump (50 ns/div.)

II FIR (50 ns/div.)

B. "LONG PULSE"

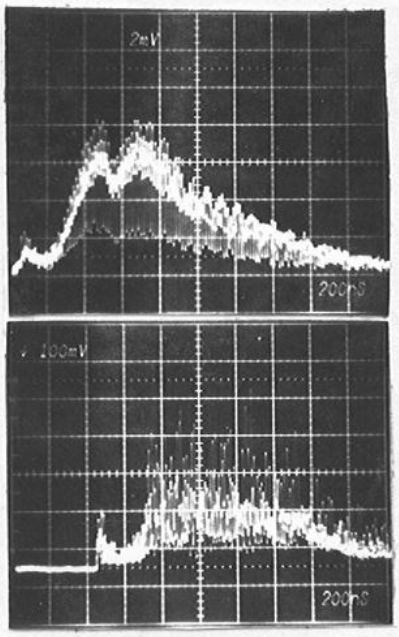

I CO_2 Pump (200 ns/div.)

II FIR (200 ns/div.)

Fig. 13 FIR and CO_2- pump pulses . L = 134 cm.

Unstable resonator.

In figure (14) we compare the FIR pump energies vs pump energy density for our linear system with the results obtained by Dodel et al. who used a "zig-zag" scheme {14}. The energies from the linear system have been normalized to the 12 cm cross-section of the zig-zag laser. The cavity losses and output coupling differ somewhat (pressures are those that give maximum output for each resonator configuration) and thus the comparison is only approximate.

We have also compared the "external" quantum efficiency vs the pump energy density for each system, figure (15). The "external" quantum efficiency, ε, is calculated by combining the ratio of FIR energy, E_{FIR}, to CO_2 pump energy, E_{CO_2}, with the Manley-Rowe limit, i.e.,

$$\varepsilon = \frac{E_{FIR}}{E_{CO_2}} \cdot \frac{\nu_{CO_2}}{\nu_{FIR}} \quad .$$

The fraction of pump energy absorbed in each oscillator configuration is shown below figure (15).

The non-linearity shown by the two longer, zig-zag pumped lasers may arise from a parasitic mode of the type shown in figure (16). Once above threshold energy loss from such a mode would increase with oscillator length and FIR gain (i.e. pump energy density). Just such behaviour is observed. The 115 cm long cavity shows a linear relation up to 1 Joule cm^{-2}, suggesting that the threshold for the parasitic mode has not yet been reached. The linearly pumped system is not susceptible to such parasitic modes and it seems reasonable to expect the linear relation between the pump and FIR energies to continue as for the shorter zig-zag laser.

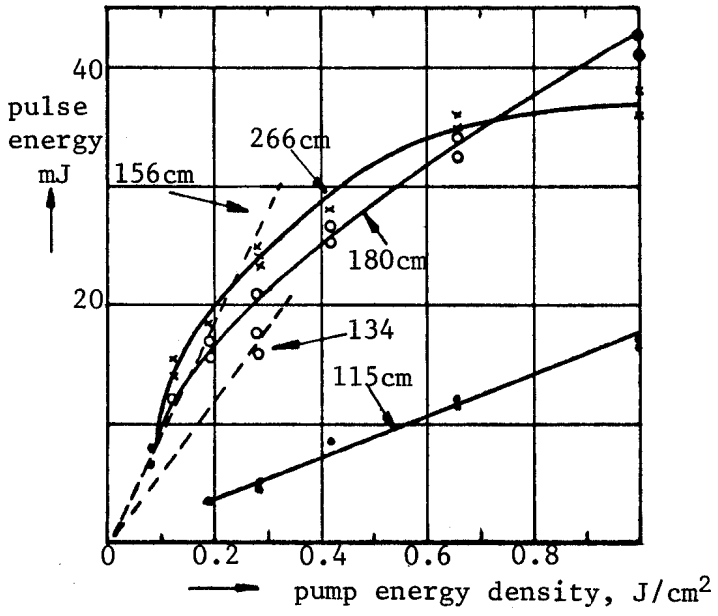

Figure 14

A comparison between FIR pulse energy as a function of the pump energy density for different oscillator lengths and pump schemes. D_2O pressure is the optimum for each resonator.

Solid lines are the results of Dodel et al. {13} using a zig-zag pump scheme, the cavity feedback being 65%. The dotted lines show the results obtained with the two linearly pumped systems described in this report. The 155 cm (plane/plane) and 134 cm long (unstable) resonators had cavity feedbacks of 27% and 32%, respectively. The cavity losses were 12%.

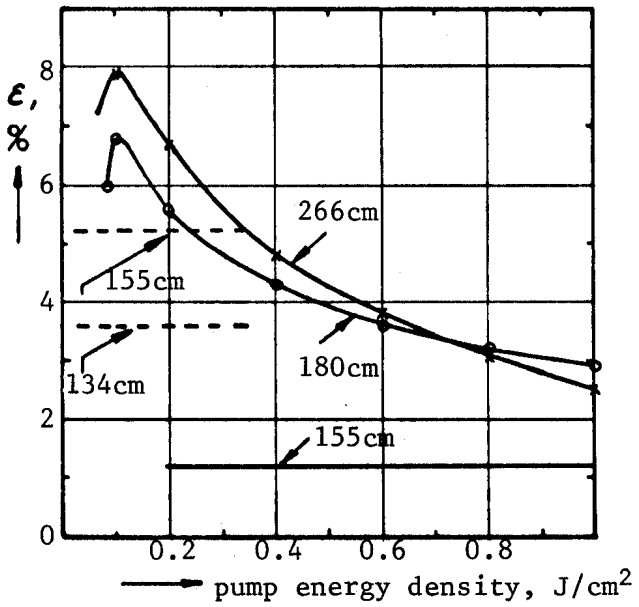

CAVITY cm	TYPE	PRESSURE (torr)	ABSORPTION %
266	ZZ	3.0	62
180	ZZ	3.5	55
*155	LP	6.5	57
134	LP	5.5	70
115	ZZ	4.5	42

* Single pass absorption

Figure 15

"External" quantum efficiency as a function of pump energy density for different oscillator lengths and pump schemes. Also shown, the fraction of pump energy absorbed for each configuration. Solid lines are the results of Dodel et al. {13} using a zig-zag pump scheme. The dotted lines are results obtained with the linear pump geometry.

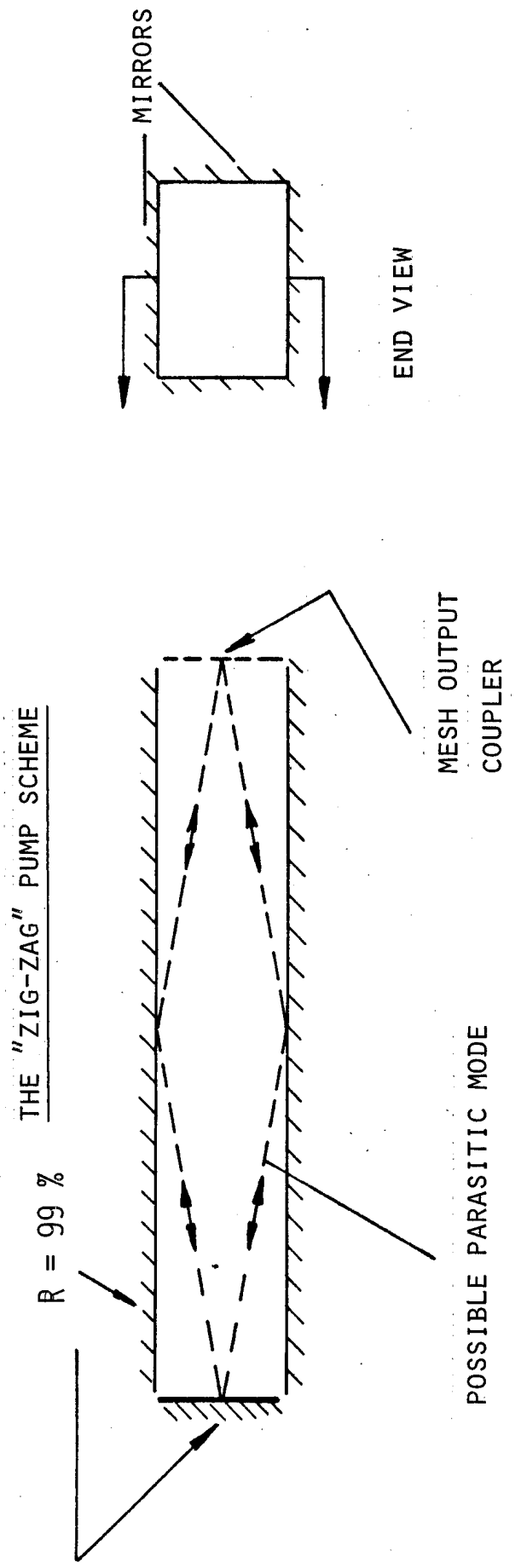

Fig. 16 A possible parasitic mode in a zig-zag pumped laser.

4. Conclusions

The excellent transmission of KCl at 9.66μm and its high reflectance at 66μm have been utilised in the design of an unstable resonator. The linear pumping scheme provides a simple but effective way of exciting large volumes and obtaining single transverse-mode operation. When D_2O vapour is optically pumped by the P(32) line of a CO_2 laser, lasing not only takes place at 66μm, but also on several refill and cascade lines, e.g. 50.5μm, 83μm and 119μm are produced. Unlike a metal mesh, whose reflectance increases rapidly with increasing wavelength, KCl has a reflection band only about 25μm wide. Thus the neighbouring lines will all be subject to a much lower feedback in the resonator. In the simple plane/plane resonator, however, both mesh and a KCl mirror are used. ASE at other wavelengths may be present and as the reflectivity of the mesh is lowered so more ASE will be measured. Thus the measured value of optimum reflectivity at 66μm, figure (7b), could be somewhat low.

We have demonstrated that the FIR output is strongly influenced, both with and without resonator feedback, by the behaviour in time of the pump pulse. For both a plane/plane and for the unstable resonator the FIR-pulse envelope exhibits a modulation that arises from both the FIR-cavity mode beating and from frequency differences that correspond to that of the CO_2 cavity-modes. The spatial {11,14} and frequency {15} dependence of the FIR pulse on the pump wave have been examined elsewhere, and it now seems clear that for efficient single-mode operation of a D_2O oscillator the CO_2 pump too must be single mode. There is little discernible difference in efficiency between long and short pulse pumping and consequently we can examine pump power scaling laws simply by varying the CO_2 pulse length (under these conditions the CO_2 laser energy remains almost constant). This is important because we wish to predict the CO_2/FIR laser parameters for high powers (1-10 megawatts), for long pulses, 0.2 - 1.5 μs duration, and with a bandwidth not exceeding 60 MHz. These specifications arise from the estimates of laser performance necessary if a scattering measurement of the ion temperature of a tokamak plasma is to be performed {16}.

Table II lists some values of oscillator and pump parameters extrapolated from our experimental results.

The 1st column summarizes the oscillator characteristics as described in this report.

The 2nd column is based on the presumption that the FIR energy will scale linearly with pump energy to a value of 0.7 J/cm^2 (i.e. an increase of x 2).

The 3rd and 4th columns retain this assumption and show the effect of modest increases in the oscillator dimensions.

The upper limit to the oscillator length arises from the need for the intermode spacing of the FIR cavity to exceed 50 MHz. This is the value of the width of the FIR gain envelope if the CO_2 pump is single mode {15}. The aspect ratio of the resonator (diameter/length) cannot be decreased indefinitely; however it appears that a ratio of 1 : 10 should be feasible {17}.

Despite expectations that increases of more than x 2 in the value of the quantum efficiency can be obtained using a single mode pump {15}, and an increase in the energy output by optimising the output coupler (ibid.) neither of these factors has been included in the calculation of table II.

Table II Simple Scaling of the FIR Laser Oscillator Based on Experimental Measurements

Oscillator Output coupling = 56% Cavity feedback = 32% Cavity losses = 12%	Present System	Scaled systems		
Diameter (cm)	6	6	8	10
Length (cm)	134	134	150	150
Area (cm^2)	28	28	50	79
Volume (litres)	4	4	8	12
Aspect ratio	1:22	1:22	1:19	1:15
Pump energy density (J/cm^2)	0.34	0.7	0.7	0.7
Cavity mode - spacing (MHz)	112	112	100	100
FIR energy density ($Jcm^{-2} \times 10^{-3}$)	1.8	3.6	3.6	3.6
CO_2 pump (in 75 ns) (J)	10	20	35	55
Fraction of pump energy absorbed (at 5.5 Torr)	70%	70%	77%	77%
FIR energy (Joules $\times 10^{-3}$) (in 75 ns)	52	104	207	323
FIR power (10^6 Watts)	0.69	1.39	2.8	4.3
CO_2 energy (J) (for 200 ns pulse)	27	53	93	147

Appendix I - Calorimetry

There is no recognized standard for calibrating calorimeters in the 50 - 500 μm wavelength region.

A comparative study of 3 pyroelectric calorimeters, a GEN TEC ED-500, a Molectron J3-05 and a Laser Precision RkP 336 was made. Good agreement between the response at 10.6 μm and that at 66 μm was found for the two former devices. The RkP gave readings 12 x higher than it should have according to its calibration factor. When the RkP was used for measurements, the calibration factor obtained using the other two detectors was used.

i.e.	GEN TEC ED 500	2.88 V/J
	Molectron J3-05*	2800 V/J
	Laser Precision RkP 336*	11.8 V/J

* with a proprietary coating to extend response in the FIR.

Appendix II - Energy Conversion Efficiency

The conversion efficiency (FIR laser energy/CO_2 laser energy) of the D_2O laser can be influenced by the past history of the laser's vacuum vessel. As an example, with a new, clean stainless steel vacuum vessel (500 litres capacity) we have observed the following behaviour:

1. Following the first filling

   The superadiant energy is low (less than 10% of the maximum possible) and the shot-to-shot conversion efficiency is erratic.

2. Following evacuation and the 2nd filling

   The FIR energy is, initially, about 85% of that possible and fairly reproducible. The average FIR energy decays, however, over a period of a few hours to its previous low value. The conversion efficiency becomes erratic.

3. Following several evacuation/refilling cycles, lasting a few days

   The maximum FIR energy is recorded and the conversion efficiency is at its most reproducible.

   If the vessel is let up to air for about 10 hours the output returns to the behaviour described in 2.

   We have observed qualitatively similar results from aluminium and from glass vessels.

This behaviour is apparently not due to a photochemical change because it is insensitive to pump dosage.

One explanation for this behaviour could be that a surface reaction takes place between the vessel and the vapour. Further reactions cease when the surfaces are sufficiently deuterated. All calorimetric measurements reported here were taken after a 'conditioning' of the vessel, and following a fresh charge of gas, or with a gentle flow of vapour through the system.

Acknowledgements

It is a pleasure to thank Professor J.C. Bünzli of the Institut de Chimie Minérale et Analytique, Université de Lausanne, who performed the measurements of the transmission of the copper meshes, Table I. We are grateful for helpful discussions with Dr. G. Dodel, Institut für Plasmaforschung, Universität Stuttgart, Dr. H. van den Bergh, Chimie Physique, Ecole Polytechnique Fédérale de Lausanne and Dr. A.C. Selden, UKAEA Culham Laboratory. The gas mix for the CO_2 laser isolation cells was optimised by M. Dupertuis, J-L. Scartezzini and R. Duperrex.
Furthermore, the authors wish to acknowledge the excellent assistance rendered by the technical services of C.R.P.P. In particular, they thank J-M. Mayor of the drawing office, R. Dussault and the staff of both the mechanical and electrical workshops and R. Gribi of the electronic laboratory.

This work was funded by the Swiss National Science Foundation and is in support of EURATOM-JET contract No B-Z-412.

TABLES

FIGURE CAPTIONS

Figure 1 — CO_2- laser system for optical pumping

Figure 2 — A typical FIR-spectrum of the isolation gas-cell mix.

Figure 3 — Some oscilloscope traces of the CO_2 laser pulse shape as a function of the time delay between firing the oscillator and the amplifiers.

Figure 4 — An unstable resonator which utilises the reststrahlen effect.

Figure 5a — Distribution of pump energy : with a reststrahlen mirror. A - A Radial variation
B - B On-axis variation

Figure 5b — Distribution of pump energy : with an opaque mirror.
A - A Radial variation
B - B On-axis variation

Figure 6 — A linearly-pumped oscillator having a reststrahlen feedback mirror.

Figure 7a — FIR energy as a function of D_2O vapour pressure : plane/plane resonator.

Figure 7b — Maximum energy output from the FIR oscillator as a function of mesh reflectivity: plane/plane resonator.

Figure 8 — FIR energy as a function of CO_2 laser pump energy for two pump durations: plane/plane resonator.

Figure 9 — A typical FIR pulse shape. Plane/plane cavity. L = 155 cm. R = 27%. 20 ns/div.

Figure 10a — FIR pulse shape : ASE

Figure 10b — CO_2 pump pulse shape
20 ns/div.
CO_2 cavity length : 240 cm

Figure 11 — FIR energy as a function of D_2O vapour pressure : unstable resonator.

Figure 12 — FIR energy as a function of CO_2 pump energy.

Figure 13 — CO_2 and FIR laser pulses. L = 134 cm.
Unstable resonator.

a. "Short pulse"
   i CO_2 pump.
   ii FIR (50 ns/div.)

b. "Long pulse"
   i CO_2 pump.
   ii FIR (200 ns/div.)

Figure 14

A comparison between FIR pulse energy as a function of the pump energy density for different oscillator lengths and pump schemes. D_2O pressure is the optimum for each resonator.

Solid lines are the results of Dodel et al. {13} using a zig-zag pump scheme, the cavity feedback being 65%. The dotted lines show the results obtained with the two linearly pumped systems described in this report. The 155 cm (plane/plane) and 134 cm long (unstable) resonators had cavity feedbacks of 27% and 32%, respectively. The cavity losses were 12%.

Figure 15

"External" quantum efficiency as a function of pump energy density for different oscillator lengths and pump schemes. Also shown, the fraction of pump energy absorbed for each configuration. Solid lines are the results of Dodel et al. {13} using a zig-zag pump scheme. The dotted lines are results obtained with the linear pump geometry.

Figure 16

A possible parasitic mode in a zig-zag pumped laser.

REFERENCES

{1} Elliott, R.J. and Gibson, A.F., Solid State Physics, (New York : Macmillan), p. 223 (1974)

{2} Green, M.R., Morgan, P.D., and Siegrist, M.R., J. Phys. E Sci.Instrum. 11, 389 (1979)

{3} Green, M.R., Kjelberg, I., Morgan, P.D., Siegrist, M.R., and Watterson, R.L., EPFL-CRPP Report, Lausanne, LRP 152/79

{4} Green, M.R., Morgan, P.D., and Siegrist, M.R., EPFL-CRPP Report, Lausanne, LRP 141/78

{5} Nicholson, J.P., and Lipton, K.S., Appl. Phys. Lett. 31, 430 (1977)

{6} Dupertuis, M.A., Scartezzini, J-L., van den Bergh, H., Dupperex R., Green, M.R., Kjelberg, I., Morgan, P.D., Siegrist, M.R., and Watterson, R.L., EPFL-CRPP Report, Lausanne, LRP 152/79

{7} Siegman, A.E., Laser Focus, p. 42, (May 1971)

{8} Hadley, G.R., IEEE, J. Qu. E. QE-10, 8, 603 (1974)

{9} a. EMI Electronics Ltd., Electron Tube Division, 243, Blythe Road, Hayes, Middx., Great Britain

b. Buckbee-Mears Co., 245 East 6th St., Saint Paul, 55101 Minnesota, U.S.A.

{10} Chantry, G.W., et al., Infr. Phys., 9, 31 (1969)

{11} Allen, L., Dodel, G., and Magyar, G., Opt. Comm. 28, 383 (1979)

{12} M.R. Siegrist, P. Gautier, M.R. Green, P.D. Morgan, J-Ch. Vittoz, and R.L. Watterson, EPFL-CRPP Report, Lausanne, LRP 145/78

{13} Lee, S.H., Petuchowski, S.J., Rosenberger, A.T. and DeTemple, T.A., Opt. Lett. 4, 6 (1979).

{14} Dodel, G., Magyar, G., and Veron D. Infr. Physics 18, 529 (1978)

{15} Woskoboinikow, P., Praddaude, H.C., Mulligan W.J., Cohn, D.R., and Lax, B., J. Appl. Phys. 50, 1125 (1979)

{16} Morgan, P.D., Green, M.R., Siegrist, M.R., and Watterson, R.L., EPFL-CRPP Report, Lausanne, LRP 154/79

{17} Selden, A.C., Private Communication, UKAEA Culham Lab